Electronic Supplementary Material (ESI) for Physical Chemistry Chemical Physics.
This journal is © the Owner Societies 2017

Supporting Information

Chiral segregation driven by a dynamical response of the adsorption footprint to the local adsorption environment: Bitartrate on Cu(110)

G.R. Darling[†], M. Forster, C. Lin, N. Liu, R. Raval[§], A. Hodgson*

Surface Science Research Centre and Department of Chemistry, University of Liverpool, Liverpool L69 3BX, UK

[†] darling@liverpool.ac.uk

[§] raval@liverpool.ac.uk

*ahodgson@liverpool.ac.uk

CONTENTS

S1. Influence of bias voltage on STM images of bitartrate on Cu(110)

Under typical imaging conditions the STM image for the bitartrate phase is well represented by the image shown in Figure 1b, characterised by trimer rows containing a central bright feature, flanked by two weaker features and separated from the next chain by bare Cu. Although the STM images are sensitive to the tip termination, see section S2 below, the images are largely insensitive to the applied bias voltage. This is illustrated in Figures S1 and S2 for two different tips. Although the contrast of the outer bitartrate relative to the central molecule is different for the two tips, the central feature always carries more intensity that the outer groups at both positive and negative bias voltages.

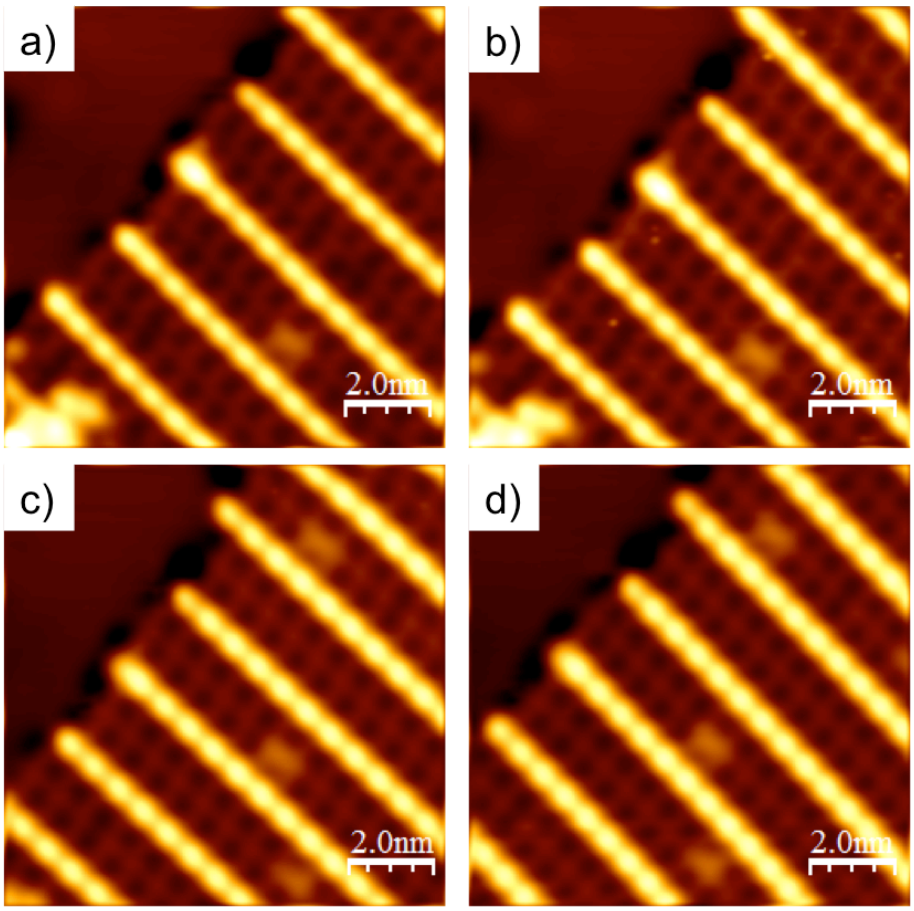

FIG. S1. STM images showing *(R,R)* bitartrate on Cu(110) showing the insensitivity to bias voltage. Tunnel conditions 100 pA and a) -400 mV, b) -200 mV, c) 200 mV and d) 400 mV respectively.

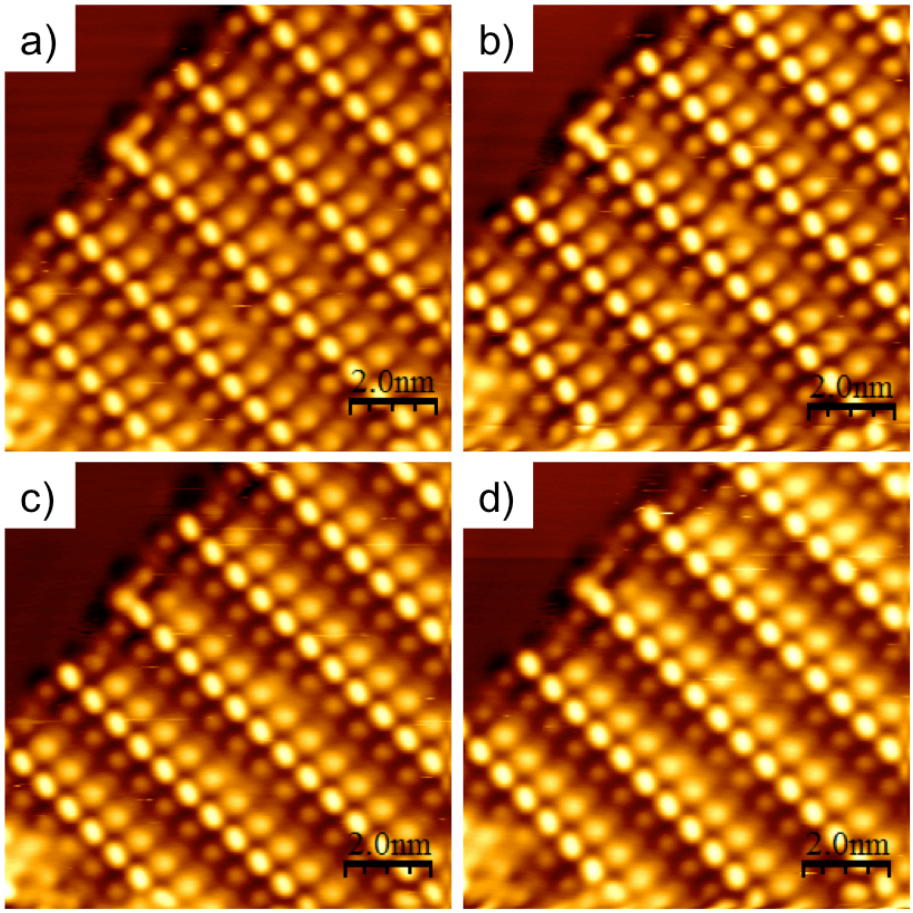

FIG. S2. Sequence of STM images showing *(R,R)* bitartrate on Cu(110) as a function of the applied bias voltage. Tunnel conditions are 100 pA and a) -400 mV, b) -200 mV, c) 200 mV and d) 400 mV respectively. The asymmetry in the trimers is associated with the tip shape and illustrates the sensitivity of the images to the tip condition, but not the bias voltage.

Figure S3 shows the IV and dI/dV behaviour of the central and outer bitartrate units. The central oblique bitartrate is always brighter than the molecules with a rectangular footprint outside it, but at negative bias the outer bitartrates become slightly more intense relative to the central feature, consistent with more distinct imaging of the trimer at negative bias. The dI/dV curves of both footprints of show a maxima near +0.2 V, which is slightly larger for the central oblique molecule. The absence of any strong bias dependence is reproduced by the Tersoff-Hamann simulations, Figure S4, which show that only for the $R_{ec}O_aR_{ec}$ arrangement does the central feature carry more intensity, and that this is insensitive to the polarity of the applied bias voltage. In contrast, different arrangements of the molecular footprint produce STM images that do not resemble the experimental images, Figure S4.

a)

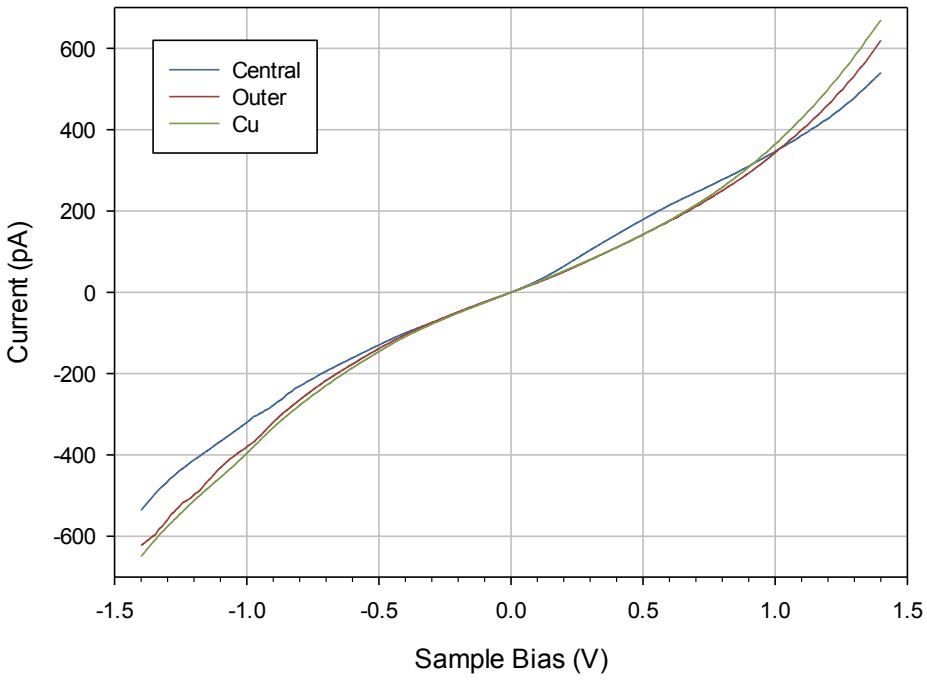

b)

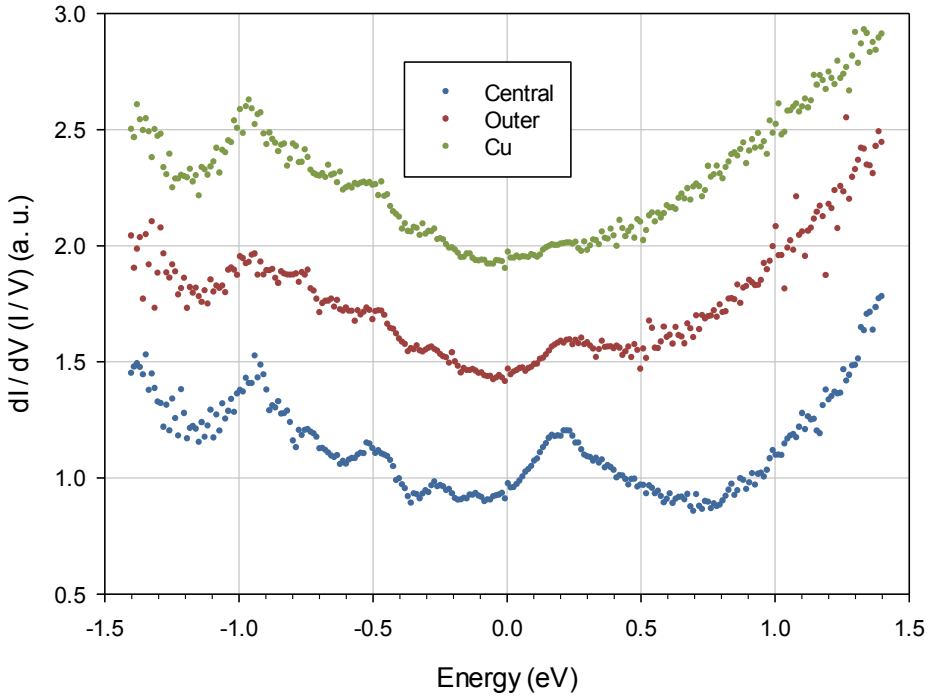

FIG. S3. (a) Tunnelling current versus sample bias for the central bitartrate, outer bitartrate and Cu terrace. The tip height for these measurements is set at the condition of -380 mV and 102 pA for each sample site. (b) Normalized scanning tunnelling spectra of central bitartrate, outer bitartrate and Cu. The curves are offset vertically by 0, 0.5, 1 respectively for visibility.

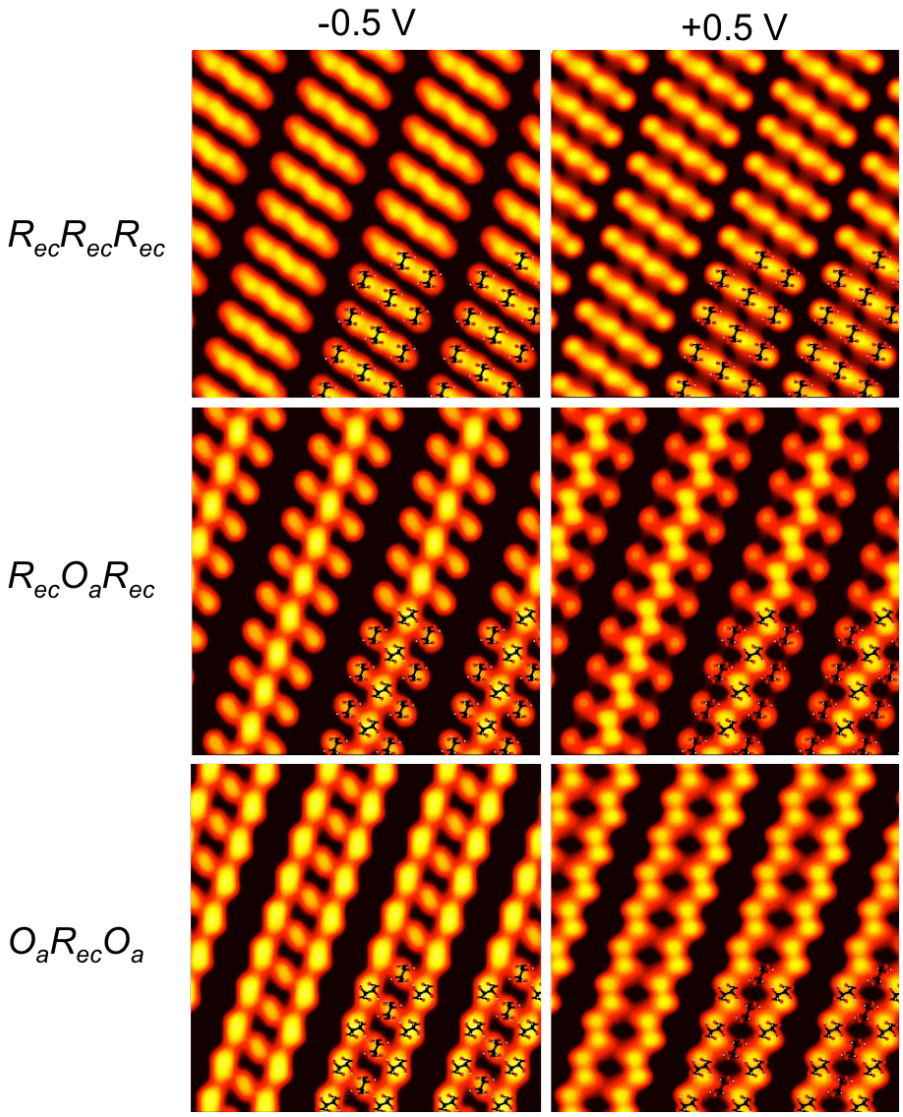

FIG. S4. Simulated STM images of bitartrate at -0.5 V and +0.5 V. Only the $R_{ec}O_aR_{ec}$ arrangement reproduces the experiment, with the central oblique bitartrate unit imaging brighter than the outer two rectangular units, irrespective of the tunnelling polarity or bias voltage. Although the simulation at +0.5 V (which does not take account of the tip convolution effects) shows a minima in the centre of the oblique bitartrate, in practice the experimental resolution was never sufficient for sub-molecular features to be seen.

S2. Tip effects in STM images of bitartrate on Cu(110)

Occasionally a tip symmetry change is observed during scanning and the contrast of the STM image changes, as shown in Figure S5. In this case the central feature of the trimer splits, with a node appearing at the position of the central feature. These images are not sensitive to the applied bias voltage and are stable until the tip is deliberately modified to return it to the usual condition (e.g. by pulsing or cleaning the tip). In the modified images the chains appear rather broad and the channel between the chains is barely resolved. Figure S6 shows a sequence of 3 images obtained during the course of such a tip change. The centre feature of the trimer splits and becomes fainter, Fig. S6b,c, and the chain appears broadened. Details of the image reflect the particular state of the tip that causes these split images (which is unknown but likely involves adsorbate decoration of the tip).

STM simulations of the $R_{ec}O_aR_{ec}$ structure (II) using a *p*-wave tip, Fig. S7, reproduce the splitting of the central bitartrate unit, placing a node in the position of the oblique molecule at the centre of the chain but leaving the outer rectangular units as maxima to create a broadened chain with a central node, similar to the images observed. Simulations for the other candidate structures (structures I and III) do not give rise to the observed splitting. The dramatic difference in the way the central bitartrate images compared to the outer units is again consistent with the central molecule adopting an oblique footprint that is different from the rectangular footprint of the neighbouring units.

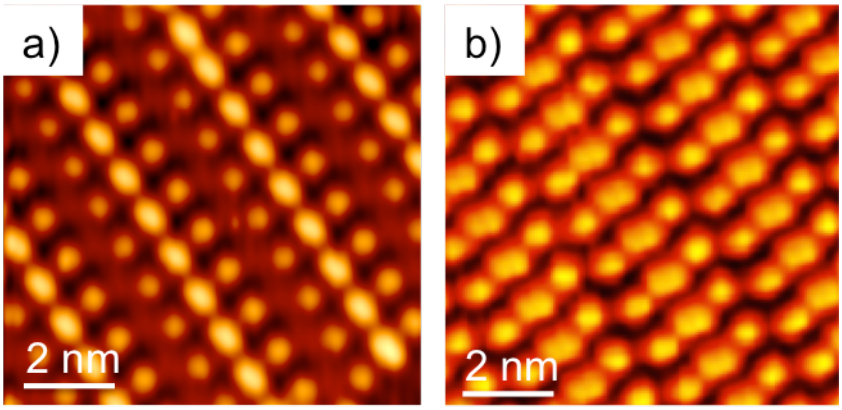

FIG S5. STM images for (S,S) bitartrate showing a) the normal image for the bitartrate phase and b) the minority, split image that appears in a small proportion of scans due to a tip change. Images taken at 300 K, a) -200 meV and 280 nA, b) -880 meV and 500 nA.

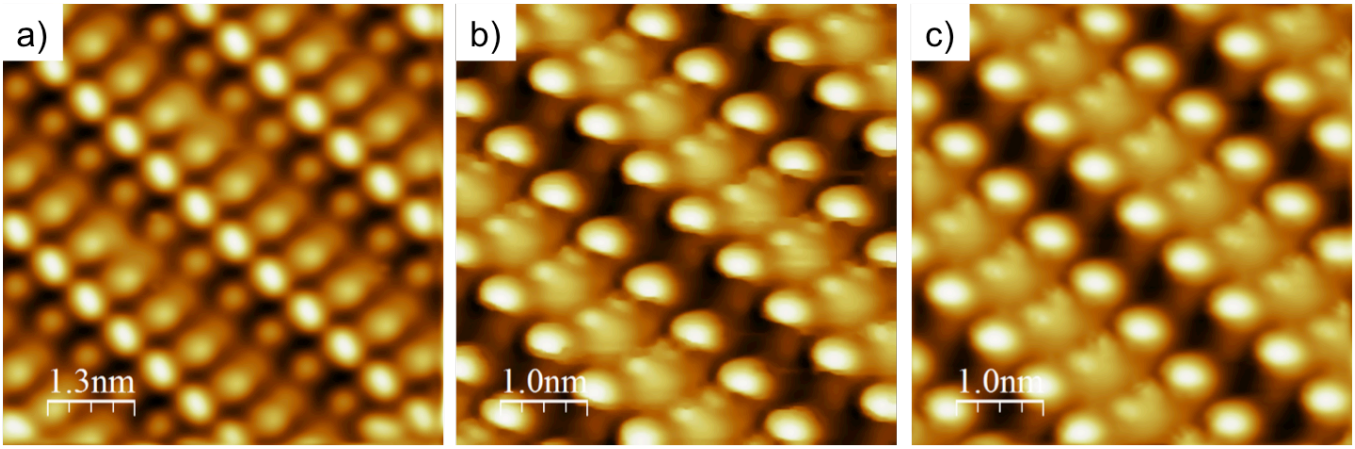

FIG S6. Sequence of STM images for a (1 2, -9 0) island of (*R,R*) bitartrate. A tip change happens between frames (a) and (b) and the image changes from the typical image (a) to the 'split' image (b, c) observed in a minority of cases due to tip decoration. Images recorded sequentially at 77 K, zooming in on the centre of frame (a). a) & b) -400 meV and 100 pA, c) -825 mV and 200 pA respectively.

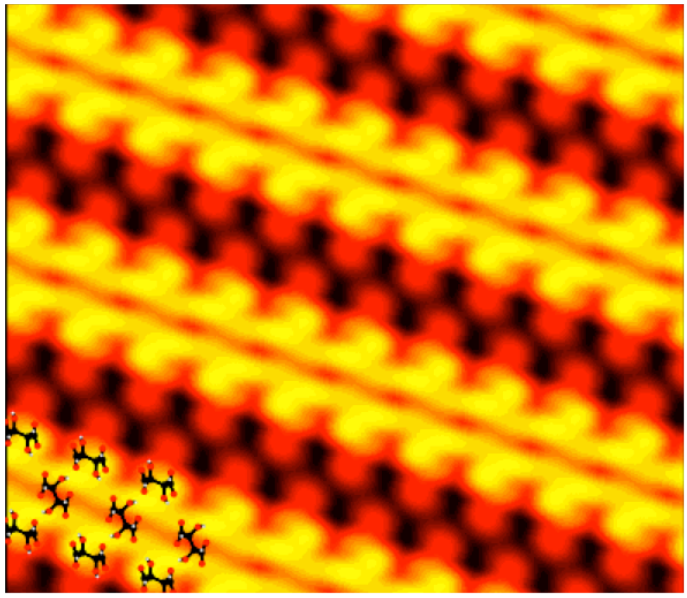

FIG. S7. Tersoff-Hamann simulation of the STM image shown in Figure S6b,c showing the splitting of the central feature of the $R_{ec}O_aR_{ec}$ bitartrate arrangement using a *p*-wave tip directed along <1-10> at -0.4 V. As for the *s*-wave tip, the simulations show no significant dependence on the bias voltage or polarity. The splitting of the central feature is large and comparable to the molecular spacing, so that the effect of a *p*-wave tip is not obscured by tip convolution effects.

S3. Calculated structures for an isolated bitartrate molecule

TABLE S1. Adsorption energy (E_{ad}) of (*R,R*) bitartrate monomers with different footprints across the Cu close packed rows, hydrogen bond length ($d_{(O\text{-}H)}$), oxygen-copper spacing ($d_{(O\text{-}Cu)}$) and the expansion of the Cu-Cu spacing beneath the carboxylate ligand ($\Delta_{(Cu\text{-}Cu)}$) in the <1-10> direction.

Footprint	E_{ad} (eV)	$d_{(O\text{-}H)}$ (Å)	$d_{(O\text{-}Cu)}$ (Å)	$\Delta_{(Cu\text{-}Cu)}$ (%)
Rectangular, R_{ec}	-2.139	2.00	1.94, 1.96	2.6
Oblique, O_a	-2.056	2.10	1.94, 1.99	2.1
Oblique, O_b	-1.720	2.86	1.93, 1.99	2.2

S4. Additional supporting calculations

TABLE S2. Comparison of the adsorption energy (E_{ad}) of (*R,R*) bitartrate in the (1 2, -9 0) unit cell calculated either with dispersion interactions (optB86b-vdW) or without (PBE).

Structure	optB86b-vdW		PBE	
	E_{ad} (eV)	ΔE_{ad} (eV)	E_{ad} (eV)	ΔE_{ad} (eV)
$R_{ec}R_{ec}R_{ec}$	-2.152	+0.123	-1.114	+0.014
$R_{ec}O_a R_{ec}$	-2.275	0.0	-1.128	0.0
$O_a R_{ec}O_a$	-2.244	+0.031	-1.073	+0.055

A comparison between the calculated binding energy of the three different arrangements when dispersion interactions are neglected, using PBE, indicates that the $R_{ec}O_aR_{ec}$ arrangement remains more stable than the other possible footprints, Table S2, although the difference in energy of the $R_{ec}R_{ec}R_{ec}$ and $R_{ec}O_a R_{ec}$ structures is greatly reduced. Previous DFT calculations [1-2], that concluded bitartrate adopted a rectangular footprint and did not form inter-molecular H-bonds, were carried out

without including dispersion interactions (using PW91) and in a smaller unit cell that prevented the mixed footprint $R_{ec}O_aR_{ec}$ trimer being found.

In order to confirm that the staggered $R_{ec}O_aR_{ec}$ arrangement does indeed form the most stable possible structure, we performed DFT calculations of a number of different possible trimer structures in the (1 2, -9 0) unit cell adopted by (*R,R*) bitartrate. The energy of structures in which bitartrate is adsorbed in an oblique arrangement are tabulated in Tables 2 and S4, and the corresponding structures are shown in Figs. 3 and S8 (see main text for discussion). In addition we investigated the formation of trimer structures oriented along <1-10> to determine if DFT correctly predicts the orientation of the bitartrate trimers and to compare to succinic acid, which orients along the <1-10> direction. The resulting adsorption geometries are shown in Fig. S9 and their adsorption energies listed in Table S3. Structure XII, which has a (*R,R*) trimer in an $R_{ec}R_{ec}R_{ec}$ arrangement oriented along <1-10>, similar to the arrangement adopted by succinic acid [3], has a higher binding energy than the structure originally proposed for bitartrate. Although the $R_{ec}O_aR_{ec}$ trimer structure oriented along <1-10> (structure XIII) is able to form hydrogen bonds between adjacent OH groups, the overall binding energy remains unfavourable.

The effect of changing the size of the bare Cu channel between the $R_{ec}O_aR_{ec}$ bitartrate chains (structure II) is listed in Table S4. Moving the bitartrate chains one unit closer together decreases the binding energy slightly, despite the more favourable van der Waals interactions, but increasing the separation further has no effect. Inserting an additional bitartrate group into the gap between the chains also destabilises the (1 2, -9 0) structure, despite creating an additional intermolecular H-bond and a higher overall density of bitartrate (Fig. S8, structure XI).

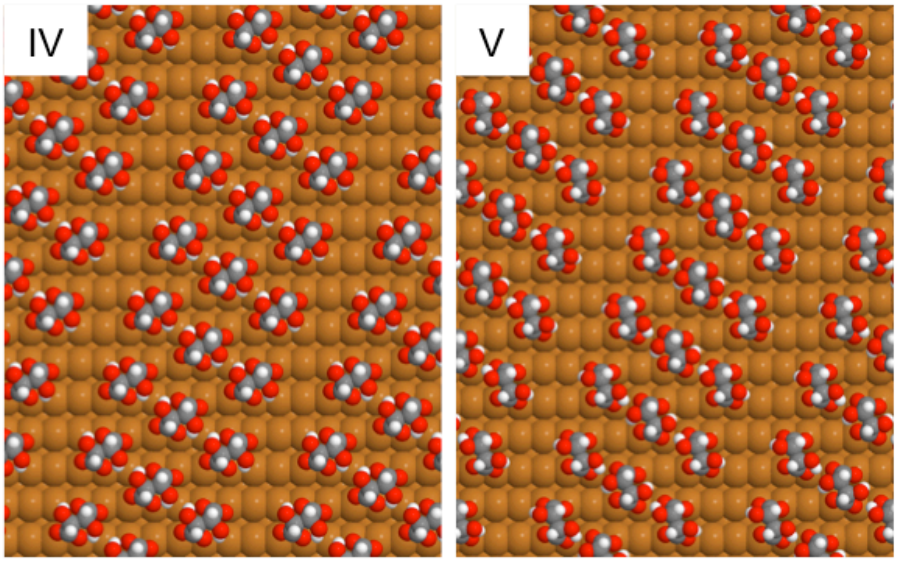

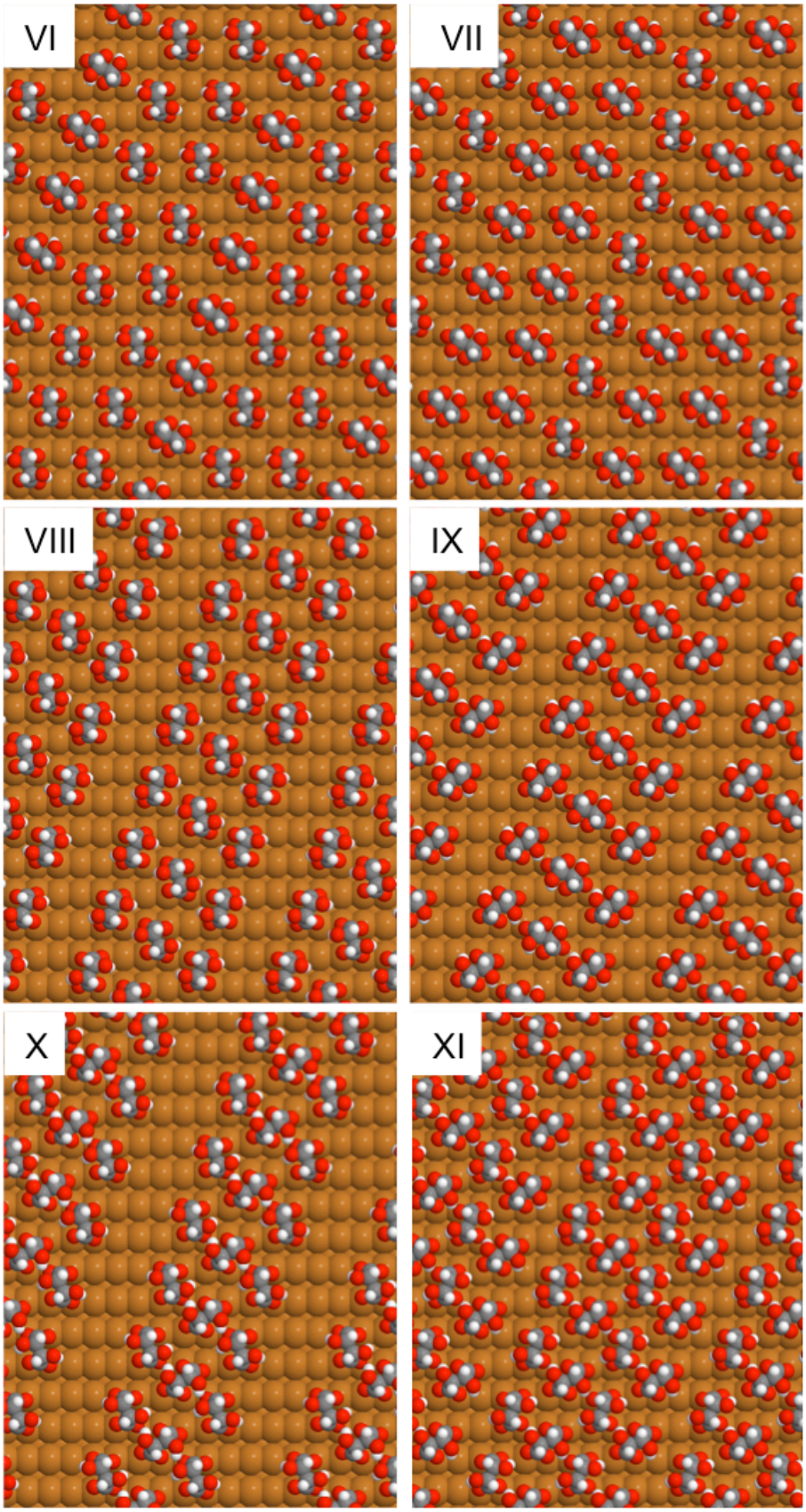

FIG. S8. Calculated minimum energy structures for the bitartrate arrangements listed in Table 2 main text. Structure XI shows the tetramer (Table S4) formed by inserting an additional molecule into the gap between the chains.

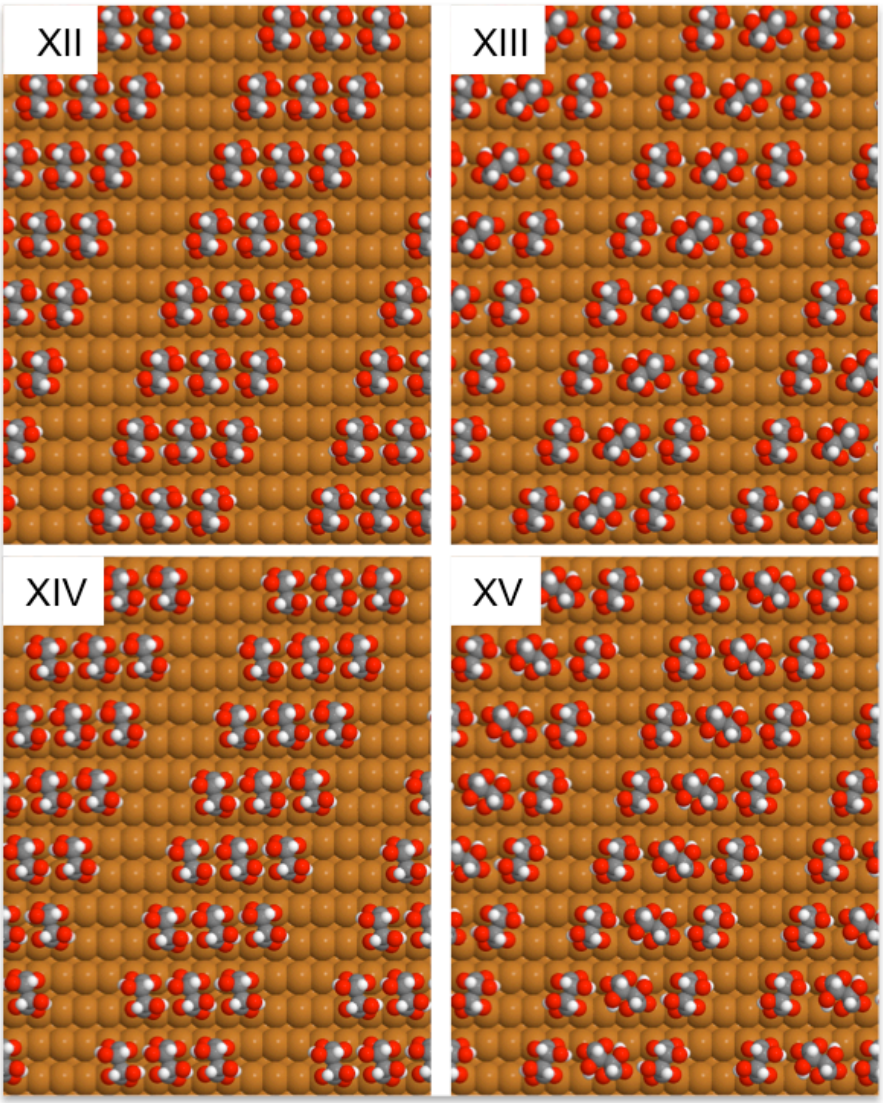

FIG. S9. Structures for bitartrate trimer chains aligned directly along <1-10>. The corresponding adsorption energies are shown in Table S3.

TABLE S3. Binding energy (E_{ad}) of (*R,R*) and (*S,S*) bitartrate trimers aligned along <1-10> in the (1 2, -9 0) unit cell adopted by (*R,R*) bitartrate. ΔE_{ad} is the binding energy relative to structure II. The corresponding structures are shown in Fig. S5.

Structure	Isomers	Footprint	E_{ad} (eV/molecule)	ΔE_{ad} (eV/molecule)
XII	(R,R) : (R,R) : (R,R)	$R_{ec}R_{ec}R_{ec}$	-2.247	0.028
XIII	(R,R) : (R,R) : (R,R)	$R_{ec}O_aR_{ec}$	-2.184	0.091
XIV	(S,S) : (S,S) : (S,S)	$R_{ec}R_{ec}R_{ec}$	-2.223	0.052
XV	(R,R) : (S,S) : (R,R)	$R_{ec}O_aR_{ec}$	-2.161	0.104

TABLE S4. Binding energy (E_{ad}) of (*R,R*) $R_{ec}O_aR_{ec}$ bitartrate trimers as a function of the chain separation and with an additional bitartrate in the gap (structure XI, Fig, S8). ΔE_{ad} is the binding energy relative to structure II. The corresponding structures are shown in Fig. 4 and Fig. S8.

Structure	Unit cell	E_{ad} (eV/molecule)	ΔE_{ad} (eV/molecule)
Fig. 4a	(1 2, -7 0)	-2.263	0.012
Fig. 4b	(1 2, -8 0)	-2.259	0.016
II, Fig. 3, 4c	(1 2, -9 0)	-2.275	0.00
Fig. 4d	(1 2, -10 0)	-2.275	0.00
XI, Fig. S8	(1 2, -9 0)	-2.258	0.017

References

1. Barbosa, L.; Sautet, P., *J. Am. Chem. Soc.* 2001, **123**, 6639-6648.
2. Hermse, C. G. M.; van Bavel, A. P.; Jansen, A. P. J.; Barbosa, L.; Sautet, P.; van Santen, R. A., *J. Phys. Chem. B* 2004, **108**, 11035-11043.
3. Liu, N.; Haq, S.; Darling, G. R.; Raval, R., *Angew. Chem., Int. Ed.* 2007, **46**, 7613-7616.